universe

MDPI

Article

A Big Bang Nucleosynthesis Consistency Test of the CCC+TL Cosmology

Rajendra P. Gupta * and Nikolaos Samaras

Department of Physics, University of Ottawa, Ottawa, ON K1N 6N5, Canada; nsamaras@uottawa.ca
* Correspondence: rgupta4@uottawa.ca

Abstract

We investigate whether Big Bang nucleosynthesis (BBN) remains compatible with the covarying coupling constants plus tired light (CCC+TL) cosmology. In this framework, only quantities with explicit length dimensionality covary through a universal scaling function $f(z)$, while dimensionless constants and dimensionless ratios remain invariant. At the redshifts z relevant to BBN, $f(z)$ approaches a constant plateau $f_{max} \simeq 3$, and the tired light contribution is negligible, so the early-time dynamics reduce to a global rescaling of dimensioned quantities. In particular, the Hubble expansion rate H at fixed temperature T satisfies $H_{CTL}(T) = f_{max}^{-1} H_{\Lambda CDM}(T)$, implying a longer cooling time Δt between weak freeze-out and the onset of nucleosynthesis by the same factor (CCC+TL labelled as *CTL*). We find that BBN predictions are preserved, provided the relevant interaction rates Γ and decay rates governing the neutron lifetime τ_n share the same plateau scaling as H, so that governing combinations such as Γ/H and $exp\left(\frac{-\Delta t}{\tau_n}\right)$ remain invariant. Implementing these plateau rescalings in the Kawano/NUC123 network (via a single control parameter fctl $\equiv f_{max}$) yields identical light-element abundances for fctl $= 1$ (ΛCDM) and fctl $= 3$(CCC+TL) to within $10^{-3} - 10^{-4}$ level, consistent with numerical rounding. We also illustrate that adopting the lower late-time CCC+TL baryon density from Pantheon+ data fit can reduce the ^{7}Li discrepancy but simultaneously increases D/H, implying that BBN alone does not select between the late-time baryon density inferences considered here.

Keywords: cosmology; theory; early universe; nucleosynthesis

1. Introduction

1.1. Big Bang Nucleosynthesis (BBN)

BBN is the earliest empirically testable episode in cosmic history, linking microphysical reaction networks to the macroscopic expansion of the universe and yielding quantitative predictions for the primordial abundances of the light nuclides D, ^{3}He, ^{4}He, and ^{7}Li. The intellectual roots of BBN trace back to the first attempts to connect the expanding, hot early universe with the formation of elements [1]. In the late 1940s, Alpher and collaborators developed the "hot big bang" nucleosynthesis picture, emphasizing thermonuclear processing in a rapidly cooling radiation bath [2,3] and extending the theoretical framework in subsequent analyses of nuclear reaction flows in an expanding medium [4]. Although the early program overreached in its aim to synthesize heavy elements, it established the central idea that the early universe would naturally produce substantial helium and trace light isotopes, while heavier elements would require stellar nucleosynthesis [5,6].

BBN became a mature quantitative theory in the 1960s and 1970s, catalyzed by the recognition that primordial helium provides a direct probe of the hot early fireball [7] and

Check for updates

Academic Editor: Pedro Pina Avelino

Received: 8 May 2026
Revised: 22 June 2026
Accepted: 23 June 2026
Published: 26 June 2026

Copyright: © 2026 by the authors. Licensee MDPI, Basel, Switzerland. This article is an open access article distributed under the terms and conditions of the Creative Commons Attribution (CC BY) license.

by the first detailed network calculations of light-element yields in standard Friedmann–Robertson–Walker cosmologies [8]. These developments were quickly integrated into a broader cosmological framework in which the expansion rate $H(T)$, the baryon-to-photon ratio η, and weak-interaction freeze-out jointly determine the neutron-to-proton ratio and thus the ^{4}He mass fraction Y_p, while deuterium and ^{3}He track the competition between nuclear burning and the declining density during expansion [9,10]. In this era, BBN also emerged as a sensitive diagnostic of new physics through its dependence on relativistic energy density ("effective number of neutrino species"), lepton asymmetry, and possible non-standard expansion histories [11–13].

A defining feature of standard BBN (SBBN) is its predictive economy: given well-measured nuclear cross-sections and standard weak rates, the primordial abundances depend primarily on η (and modestly on the radiation content and neutron lifetime) [14–16]. The reliability of these predictions rests on continued progress in nuclear inputs and neutrino-decoupling physics, including refined thermonuclear reaction rate compilations and sensitivity studies [17–20] and improved treatments of non-instantaneous neutrino decoupling and QED plasma effects [21,22]. Parallel to these theoretical advances, community codes and benchmarks were developed to propagate nuclear and cosmological uncertainties into abundance predictions, from early implementations to widely used public calculations [23–26].

Observationally, BBN is relevant because it anchors the cosmic baryon density and provides a stringent consistency check across epochs: η inferred from primordial deuterium in metal-poor absorbers [27–30] can be directly compared to the baryon density independently inferred from cosmic microwave background (CMB) anisotropies [31,32]. This BBN–CMB concordance has become a cornerstone of the standard cosmological model and a powerful lever arm for constraining extensions such as extra relativistic species or altered early-time expansion [33–36]. Primordial ^{4}He, inferred from recombination-line spectroscopy of low-metallicity H II regions, provides complementary sensitivity to the expansion rate and lepton asymmetry [37–39]. Together with deuterium, helium locks down the thermal history of the first minutes and quantifies the allowed room for beyond-standard-model effects.

Despite these successes, BBN also highlights persistent tensions that motivate renewed theoretical scrutiny. Most notably, the long-standing "lithium problem"—the discrepancy between SBBN predictions and the lower ^{7}Li abundances observed in metal-poor halo stars—has stimulated extensive work on stellar depletion, nuclear systematics, and new-physics remedies [34,40–43]. Thus, BBN remains simultaneously a triumph of early-universe physics and an active testing ground: it connects particle interactions, nuclear astrophysics, and cosmology, and it supplies one of the most sensitive probes of any model that modifies reaction kinetics, the expansion rate, or the mapping between temperature and time in the pre-recombination universe [33,35,36].

In summary, BBN provides one of the earliest and most stringent probes of cosmology, linking microphysical processes at temperatures T $\sim$ 0.01–10 MeV to present-day light-element abundances. In the standard ΛCDM framework, BBN predictions depend primarily on the baryon-to-photon ratio η, the Hubble expansion rate $H(T)$, and well-measured weak and nuclear reaction rates [23,44–46].

1.2. Covarying Coupling Constants (CCC)

The covarying coupling constants framework traces its lineage to ideas in Dirac-style cosmology: Dirac's proposal that the strengths of gravity and electromagnetism may evolve in a correlated way, together with the broader point—emphasized in later work—that allowing one dimensionful constant to vary generally implies that other dimensionful

constants cannot consistently remain fixed. In CCC, this logic is taken seriously while keeping dimensionless constants (for example, the fine-structure constant) outside the scope of the principle.

Historically, the conceptual thread begins with Dirac (1937) [47] and continues through early developments by Gilbert [48,49] and by Canuto & Londenquai [50], who explored cosmological consequences of evolving constants in generalized Dirac frameworks. In the decades since, a number of mathematically adjacent approaches have appeared. Of particular relevance are scale-invariant vacuum cosmologies developed by Bouvier (summarized in Maeder 2023 [51]) and by Maeder [52,53], where effective time dependence in gravitational strength (and, in their formulations, the fine-structure constant as well) arises via Weyl-integrable rescalings of the metric. While the underlying motivations differ from CCC, these theories likewise introduce non-trivial temporal evolution in gravitational coupling that can lead to phenomenology reminiscent of CCC-induced modifications to Friedmann evolution. Building on this general lineage, the CCC program pursued here frames the co-evolution of dimensionful constants through a single governing function $f(t)$, showing how such correlated rescalings can yield effective contributions that behave like dark matter and dark energy across cosmological and astrophysical settings.

Time-variable G scenarios have also been widely investigated in scalar–tensor gravity, most notably, the Jordan–Brans–Dicke theory [54]. CCC overlaps with these models only at the broad level of permitting a dynamical gravitational coupling: structurally, CCC does not attribute the variations of G, c, h, and related constants to a new scalar degree of freedom with a canonical kinetic term. Instead, CCC proceeds phenomenologically, guided by dimensional consistency and local conservation principles, producing a distinct pattern of modifications to Einstein–Friedmann dynamics. In parallel, Weyl-based constructions—Weyl's original geometry and later Weyl-integrable formulations [50,55,56]—also employ non-Riemannian structure to generate effective rescalings of physical units. CCC does not assume Weyl gauge symmetry or non-metricity, but the resulting effective behavior of the gravitational coupling can appear superficially similar in certain regimes. In this sense, CCC occupies a complementary niche: neither a Jordan–Brans–Dicke scalar–tensor model nor a Weyl-integrable geometric reformulation, but a correlated-variation framework in which dimensionful constants evolve together. An action-based perspective connecting $c(t)$ and $G(t)$ has been developed elsewhere [57].

Finally, it is worth noting that the literature placing empirical bounds on variations of G, c, and other dimensionful parameters is extensive, spanning laboratory, Solar System, stellar, pulsar-timing, and cosmological probes. A key interpretive point for CCC, however, is that many such constraints are formulated within a "single-varying-constant" paradigm: one parameter is permitted to drift while others are implicitly held fixed. Citations for the G variation studies include [58–82]. Among others, the potential variation of c has been studied by [83–92]. From the CCC viewpoint, these studies effectively set the common scaling function to unity by assumption, precluding the correlated evolution that CCC posits and rendering "one-constant-at-a-time" interpretations potentially misleading when translated into a covarying framework.

1.3. CCC+Tired Light (TL) Phenomenology

Tired light limitations that led to the rejection of this concept, such as Compton scattering, time dilation, Tolman brightness test, and the CMB isotropy, do not apply, as discussed in earlier papers [93–97] primarily because the tired light effect exists in parallel with the universe's expansion.

In the CCC framework, this tired light component is not an ad hoc phenomenological term, but a manifestation of an underlying vacuum microstructure that co-determines the

fundamental *dimensionful* constants. The vacuum is treated as a medium with microscopic degrees of freedom, described by a coarse-grained order parameter $\Phi(t)$, through which photons propagate and lose an infinitesimal fraction of their energy in a non-scattering, non-dispersive way, while the universe also expands. The same microstructure governs the effective speed of light $c(t)$ and gravitational coupling $G(t)$, so that they become functions of $\Phi(t)$, whereas dimensionless constants such as the fine-structure constant α remain strictly invariant.

A related but distinct approach to photon propagation in a structured vacuum is provided by deconfining SU(2) Yang–Mills thermodynamics, in which coarse-graining over microscopic non-Abelian degrees of freedom gives rise to a thermal ground state and supports electromagnetic disturbances with wave-like or photon-like behavior [98,99]. The CCC+TL model considered here is not intended as a realization of that SU(2) framework, and the order parameter $\Phi(t)$ introduced above should not be identified with the SU(2) Yang–Mills thermal ground state. Rather, CCC+TL is a phenomenological covarying-constant model in which dimensionful quantities scale coherently through a universal function $f(t)$, while dimensionless constants and dimensionless ratios remain invariant. The distinction is particularly important for the present BBN test: during the BBN epoch, f(z) lies on its asymptotic plateau and is effectively constant. Thus, the calculation does not require a rapidly varying (T) during nucleosynthesis; it tests whether the plateau scalings preserve the dimensionless reaction-to-expansion and decay-to-cooling combinations that determine the light-element abundances.

A key structural ingredient of CCC is the invariant ratio $G/c^3 = \gamma$, motivated by the form of the Einstein–Hilbert action, which requires the prefactor c^3/G to be time-independent if the gravitational field equations are to retain their standard form. This motivates a scaling ansatz in which only quantities with non-zero length dimensionality vary: if a quantity X has length dimension L^n, then $X(t) = X(0)f^n(t)$ for some dimensionless microstructural scaling function $f(t)$. A simple realization is $c(t) = c(0)f(t)$, $G(t) = G(0)f^3(t)$, $\hbar(t) = \hbar(0)f^2(t)$, and $k_B = k_B(0)f^2(t)$, so that G/c^3 is constant, and Planck units acquire a natural microscopic interpretation. The length dimensionality rule is modified slightly for the expressions involving time differentiation or integration, such as for the Hubble rate with no length dimension scaling as $f(t)^{-1}$ as shown below.

This microstructure admits a Kaluza-type geometric reading in which $\Phi(t)$ plays the role of an effective extra dimension whose geometry co-determines both light propagation and gravitational strength, echoing earlier unification attempts in higher-dimensional and induced-gravity theories [100–103]. An important conceptual consequence is that observational tests that vary only a single constant while holding all others fixed are inconsistent with any such co-varying-constant framework: fixing one dimensionful constant freezes the underlying degree of freedom and therefore forces all dependent constants to be constant by construction [104–106]. CCC therefore promotes a more coherent analysis in which the expansion rate, the tired light contribution, and the co-variation of $c(t)$, $G(t)$, $\hbar(t)$, and $k_B(t)$ are treated consistently, while α and other dimensionless couplings remain unchanged (Cuzinatto et al., 2026b) [97].

BBN is one of the most essential tests to pass for any new cosmology model. The CCC+TL model modifies cosmology by allowing dimensional constants to covary with cosmic time while preserving dimensionless constants and ratios. It also replaces dark matter and dark energy with modified distance–redshift relations and a revised definition of the critical density. Given these departures, it is natural to ask whether CCC+TL alters the successful ΛCDM BBN predictions.

The covarying coupling constant plus tired light model has already been successful in alleviating the 'impossible early galaxy problem' and fitting the SNe Ia Pantheon+ data [107].

Additionally, it is consistent with (a) the BAO and CMB sound horizon observations [108], (b) galaxy formation time scales at cosmic dawn and time dilation [109], (c) galaxy rotation curves and galaxy cluster dynamics [110], (d) mass, size, density, and luminosity evolution of galaxies [109], (e) gravitational lensing and DESI findings of increasing dark energy density with redshift [109], and cosmic chronometer compatibility [110].

This paper is structured as follows: Section 2 presents key features of the of CCC+TL model relevant for BBN; in Section 3 we discuss the ingredients of BBN; Section 4 is devoted to the nuclear reaction rates and neutron lifetime; Section 5 details the testing of the new model with a modified Kawano/NUC123 code; Section 6 is used for discussion; and Section 7 provides the conclusion.

2. Key Features of the CCC+TL Model Relevant for BBN

The CCC+TL model has been extensively discussed and applied to multiple cosmological and astrophysical observations in several papers mentioned above. Thus, in this section, we will discuss the model features that are directly relevant to BBN.

2.1. Covarying Coupling Constants

Derived from local energy conservation laws applied to exploding stars [101], they can be considered as a generalization of Dirac's large number hypothesis [47] that predicted the evolution of the gravitational constant with cosmic time. In CCC+TL, any quantity X with net length dimensionality n scales as

$$X(z) = X_0 f(z)^n, \tag{1}$$

where $f(z)$ is a universal scaling function. Examples include:

- Speed of light: $c \sim f\ (n = 1)$;
- Newton constant: $G \sim f^3\ (n = 3)$;
- Planck constant: $\hbar \sim f^2\ (n = 2)$;
- Boltzmann constant: $k_B \sim f^2\ (n = 2)$.

Thus, dimensionless constants such as the fine-structure constant, mass, charge, gauge couplings, etc., are invariant in the CCC+TL cosmology. Ratios of dimensioned quantities are dimensionless, so they do not evolve. At high redshifts corresponding to BBN and recombination, $f(z)$ assumes its asymptotic constant value of approximately 3, depending on the observational data fit of the late universe or recombination. Thus, all dimensional scalings reduce to fixed multiplicative factors. Mass and charge do not evolve since they have no length dimension. The premise here is that as the universe expands at a macroscopic scale, it affects the measurement unit of length at the microscopic scale.

2.2. Expansion History

Despite its conceptual differences from the ΛCDM model, the CCC+TL expansion rate at high redshifts is proportional to the ΛCDM model, i.e., for the radiation-dominated Friedmann universe given by the Hubble parameter $H(T)$ at temperature T,

$$H_{CTL}(T) \propto H_{\Lambda CDM}(T). \tag{2}$$

Here, CCC+TL is abbreviated as CTL.

Friedmann equation and continuity equation in a flat universe for the two models are as follows [107].

2.3. ΛCDM Model

$$H^2 = \frac{8\pi G_0}{3c_0^2}\left(\varepsilon_{m,0}(1+z)^3 + \varepsilon_{r,0}(1+z)^4\right) + \frac{\Lambda}{3}, \tag{3}$$

$$\dot{\varepsilon} + 3\frac{\dot{a}}{a}(\varepsilon + p) = 0. \tag{4}$$

Here, the scale factor is a, the current energy densities are $\varepsilon_{m,0}$ for matter and $\varepsilon_{r,0}$ for radiation, and pressure is p, with a related to the observed redshift z via $a = \frac{1}{(1+z)}$.

2.4. CCC Model

$$(H+\alpha)^2 = \frac{8\pi G_0}{3c_0^2}\left(\varepsilon_{m,0}(1+z)^3 f(z)^{-1} + \varepsilon_{r,0}(1+z)^4 f(z)^{-2}\right), \tag{5}$$

$$\dot{\varepsilon} + (3H+\alpha)\varepsilon + 3(H+\alpha)p = 0. \tag{6}$$

Here α is a constant defining the variation of the constants through $f(t) = exp\ (\alpha(t - t_0))$ with t_0 being the current time. Since H increases rapidly with the redshift, α can be neglected in Equation (5) for high redshift, early universe studies. The same is true about the continuity equation, Equation (6); it becomes the same as Equation (4).

Comparing Equations (3) and (5) in the radiation-dominated universe, we see $H_{CCC} = f(z)^{-1} H_{\Lambda CDM}$. Since $f(z)$ asymptotically approaches a maximum value f_{max}, and since cosmic temperature evolves as $(1+z)$, we get $H_{CCC}(T) = f_{max}^{-1}$.

2.5. CCC+TL Model

The treatment of this model comprises expressions involving tired light [98]:

$$\int_0^{z_c} \frac{dz}{(H_{c,0}+\alpha)(1+z)^{(\frac{3}{2})} f(z)^{-(\frac{1}{2})} - \alpha} - [H_{t,0}]^{-1} ln\left[\frac{1+z}{1+z_c}\right] = 0\,. \tag{7}$$

Rewriting it,

$$\begin{aligned}(1+z) &\equiv (1+z_c)(1+z_t)\\ &= (1+z_c)\ exp\left(H_{t,0}\int_0^{z_c} \frac{dz}{(H_{c,0}+\alpha)(1+z)^{(\frac{3}{2})} f(z)^{-(\frac{1}{2})} - \alpha}\right).\end{aligned} \tag{8}$$

Here, $H_{c,0}$ is the Hubble constant corresponding to CCC and $H_{t,0}$ to TL with $H_0 = H_{c,0} + H_{t,0}$, with z_c the CCC expanding Universe redshift and z_t due to TL. $H_{t,0}$ is related to $H_{c,0}$ through

$$H_{t,0} = \frac{(H_{c,0}+\alpha)}{2}\left(3 + \frac{\alpha}{H_{c,0}}\right). \tag{9}$$

The exp factor in Equation (8) represents the tired light redshift $(1+z_t)$. The free parameters $H_{c,0}$ and α are determined by fitting the Pantheon+ data [107] and, alternatively, by fitting the CMB sound horizon angle [108]. Its behavior is shown in Figure 1. Tired light has no effect at the BBN epoch. Therefore, we can use the same expressions for CCC+TL as for CCC; as in the case of CCC, $f(z)$ asymptotically approaches a maximum value f_{max}—approximately 3, depending on the values of the parameters H_0 and α determined by fitting observational data such as Pantheon+ [111,112], as shown in Figure 2.

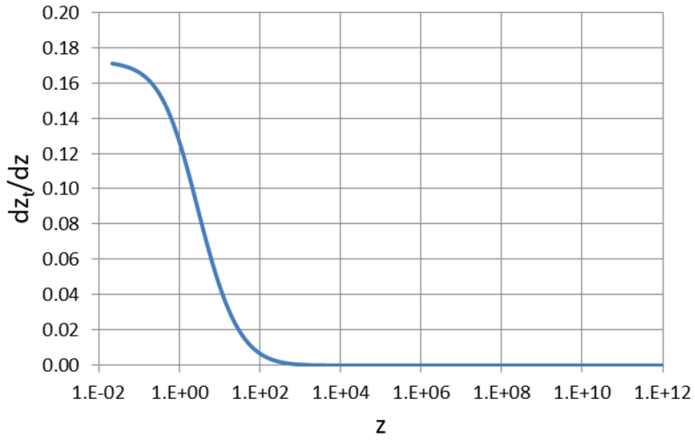


Figure 1. The tired light contribution to the observed redshift with typical H_(c,0) and α parameters. It shows a complete absence of the tired light effect at the BBN epoch.

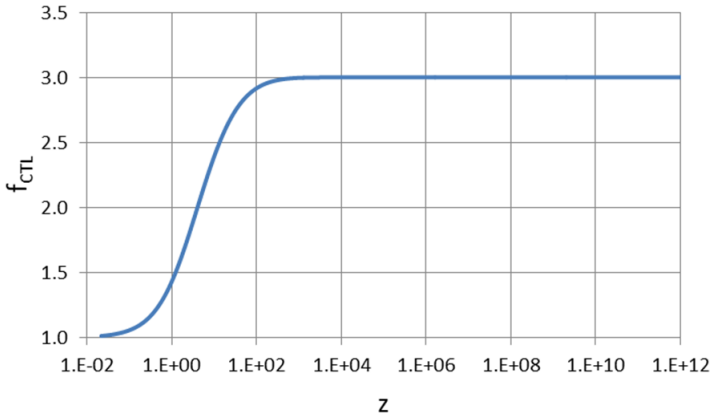


Figure 2. Variation of the function f with z. It has a fixed value, f_{max}, at BBN redshifts.

As shown in an earlier paper [108], the temperature T in the CCC+TL model evolves as $(1+z)$, i.e., the same as in the ΛCDM and CCC models. We can therefore conclude that $H_{CTL}(T) = f_{max}^{-1} H_{\Lambda CDM}(T)$ at the BBN epoch, as shown in Figure 3.

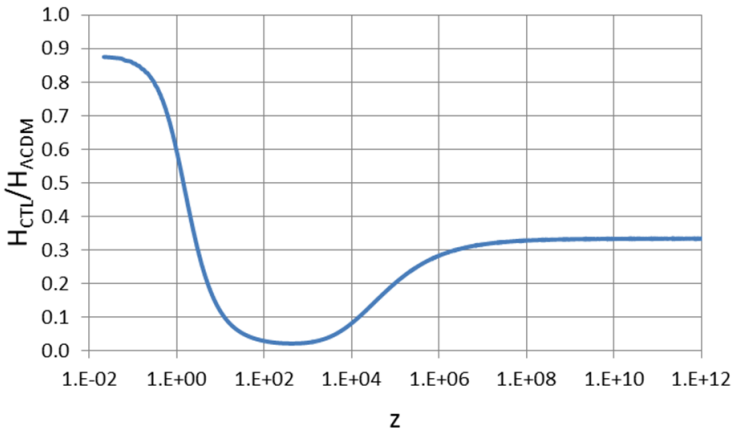


Figure 3. Variation of $H_{CTL}/H_{\Lambda CDM}$ with z. The ratio has a fixed value, $1/f_{max}$, at BBN redshifts.

We also determined the evolution of cosmic time (age of the universe) with redshift. It is shown in Figure 4 as a ratio of $t_{CTL}/t_{\Lambda CDM}$, which approaches a constant value f_{max}.

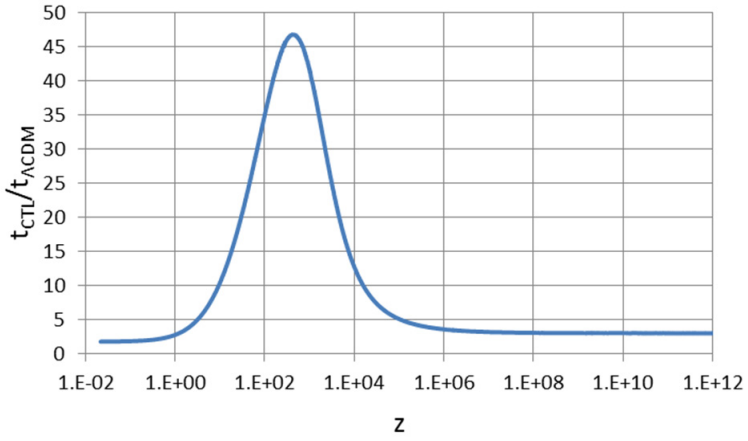


Figure 4. Variation of $t_{CTL}/t_{\Lambda CDM}$ with z. The ratio has a fixed value, f_{max}, at BBN redshifts.

2.6. Critical Density and Baryon Density Today

In a flat CCC+TL universe without dark matter or dark energy, the critical density is defined as

$$\varepsilon_{c,0}^{CTL} = \frac{3c_0^2(H_{c,0}+\alpha)^2}{8\pi G_0} = \frac{(H_{c,0}+\alpha)^2}{H_0^2}\varepsilon_{c,0}^{\Lambda CDM}. \tag{10}$$

Considering that from Pantheon+ data, $H_{c,0} = 59.5\ \mathrm{kms}^{-1}\mathrm{Mpc}^{-1}$, $\alpha = -0.80H_{c,0}$, and $H_0 = 73.0\ \mathrm{kms}^{-1}\mathrm{Mpc}^{-1}$, we get $\varepsilon_{c,0}^{CTL} = 0.027\ \varepsilon_{c,0}^{\Lambda CDM}$. If we consider the same parameters at recombination, i.e., $H_{c,0} = 59.5\ \mathrm{kms}^{-1}\mathrm{Mpc}^{-1}$, $\alpha = -0.75H_{c,0}$, and $H_0 = 67.4\ \mathrm{kms}^{-1}\mathrm{Mpc}^{-1}$, we get $\varepsilon_{c,0}^{CTL} = 0.048\ \varepsilon_{c,0}^{\Lambda CDM}$. It means that the critical energy density in the CCC+TL cosmology is in the range of the baryon energy density in the ΛCDM. Since the photon energy density is determined by the cosmic microwave background temperature of 2.7255 K, it yields the same photon energy density in both models. And, since number density, n, evolution is the same for baryons and photons when the total number of each is conserved, we get $\eta \equiv \frac{n_b}{n_\gamma}$ for the CCC+TL model, ranging from 56% to 100% of its ΛCDM value of $\cong 0.048\ \varepsilon_{c,0}^{\Lambda CDM}$.

3. Ingredients of BBN

BBN predictions depend on the following dimensionless or effectively dimensionless quantities:

1. *Baryon-to-photon ratio*

$$\eta = \frac{n_b}{n_\gamma}. \tag{11}$$

This is the dominant parameter controlling the abundances of deuterium and other light elements. As discussed above, it can differ in the CCC+TL model by a factor of 0.56 or more compared to ΛCDM.

2. *Expansion-to-reaction-rate ratios,*

$$\frac{\Gamma_{n\leftrightarrow p}(T)}{H(T)}. \tag{12}$$

where $\Gamma_{n\leftrightarrow p}$ denotes the weak interconversion rate between neutrons and protons.

3. *Energy ratios:*

The ratios, such as binding energies relative to thermal energy, e.g., $\frac{B_D}{k_B T}$ for deuterium formation, where B_D is the deuterium binding energy, do not change between the

two models as they are dimensionless; as discussed above, dimensionless quantities and dimensionless ratios of dimensioned quantities do not evolve in the CCC+TL cosmology.

4. *Neutron lifetime:*

The neutron lifetime determines the fraction of neutrons after freeze-out (temperature too low for thermal equilibrium) that are able to form He and other light elements.

BBN does not depend directly on present-day density parameters such as ε_b, except insofar as they map onto η.

4. Weak Interaction Rates and Neutron Lifetime

4.1. Neutron–Proton Interconversion Rate

It can be written schematically as [15,113,114]

$$\Gamma_{n\leftrightarrow p}(T) \propto G_F(t)^2 T^5 \times F\left(\frac{\Delta m_{np} c^2}{k_B T}\right). \tag{13}$$

where $G_F(t)$ is the Fermi constant (potentially time-dependent in a general theory), Δm_{np} is the neutron–proton mass difference, F is a dimensionless phase-space function. In a pedagogical approach, we may write it as neutrinos and antineutrinos mediating the back-and-forth conversion of protons and neutrons via the weak nuclear force: $\Gamma_{n\leftrightarrow p} = n_\nu c \sigma_w$. Here n_ν is the neutrino number density and σ_w is the weak-interaction cross-section. Multiplying and dividing the right-hand side by the neutrinos' energy E_ν, we may write $\Gamma_{n\leftrightarrow p} = \varepsilon_\nu c \sigma_w / E_\nu$. Considering that neutrinos are relativistic particles, their energy density $\varepsilon_\nu \sim f^{-2}$ (see Equation (5)) and energy $E_\nu \sim f^2$. With $c \sim f$ and $\sigma \sim f^2$, we can write $\Gamma_{n\leftrightarrow p} \sim f_{max}^{-1}$. Thus,

$$\left[\frac{\Gamma_{n\leftrightarrow p}(T)}{H(T)}\right]_{CTL} = \left[\frac{f_{max}^{-1}\Gamma_{n\leftrightarrow p}(T)}{f_{max}^{-1}H(T)}\right]_{\Lambda CDM} = \left[\frac{\Gamma_{n\leftrightarrow p}(T)}{H(T)}\right]_{\Lambda CDM}. \tag{14}$$

This is then compliant with the dimensionality rule discussed above involving relativistic particles. We conclude that BBN is unaffected due to the expansion-to-reaction rate ratio. In other words, the reaction rates follow the Hubble expansion rate. We may generalize it as an ansatz to all rates, such as interaction and decay rates, that they have a scaling symmetry consistent with the Hubble expansion rate.

4.2. Deuterium Bottleneck–Neutron Survival

Formation of deuterium is the crucial step in the synthesis of elements from protons and neutrons. An excessive number of high-energy photons at high temperatures quickly photodissociate newly formed deuterium, which is essential for the formation of helium and other elements. However, the Hubble expansion cools the universe, and at about 0.1 MeV (T_{BBN}), the energetic photon numbers are reduced enough to allow the formation of such elements. But the lifetime of neutrons of about 880 s (τ_n) leads to not all neutrons at freeze-out being available to form elements. The cooling time Δt_{cool} from freeze-out to T_{BBN} is thus crucial in determining the fraction of neutrons forming the element through the proportionality factor $exp\left(\frac{-\Delta t_{cool}}{\tau_n}\right)$.

The temperature in the expanding universe in the CCC+TL and ΛCDM models is given by

$T = T_{CMB}(1+z) = T_{CMB}/a$, i.e.,

$$\frac{dT}{dt} = -\frac{\dot{a}}{a^2} T_{CMB} = -H T_{CMB}(1+z). \tag{15}$$

Since, as shown above, $H_{CCC}(T) = f_{max}^{-1} H_{\Lambda CDM}(T)$, for the same dT, $dt_{CTL} = f_{max} dt_{\Lambda CDM}$. Thus, a reduced Hubble expansion rate by a factor f_{max} means a longer cooling time by the same factor and a concomitant reduction in Helium formation.

The above expression (Equation (15)) assumes the standard CCC+TL temperature–redshift relation

$$T = T_0 \, (1 + z). \tag{16}$$

It is useful to comment on how the result would change if one adopted an alternative high-temperature CMB relation, such as

$$\frac{T}{T_0} = \nu_{CMB}(1 + z), \, \nu_{CMB} \simeq 0.63, \tag{17}$$

as proposed in an SU(2) Yang–Mills thermodynamic treatment [115]. For a constant asymptotic coefficient ν_{CMB}, BBN at a fixed physical temperature would occur at a redshift larger by $1/\nu_{CMB}$, but the differential cooling equation would still satisfy

$$\frac{dT}{dt} = -HT. \tag{18}$$

Therefore, at fixed physical temperature and fixed baryon-to-photon ratio η, the internal CCC+TL plateau-scaling argument developed here would remain unchanged. The more significant effect would arise in the mapping between present-day density parameters and the physical η during BBN. If baryon number conservation were combined with such a modified photon temperature normalization, the photon number density would scale as ν_{CMB}^3, so the inferred η could shift by a factor of order

$$\nu_{CMB}^{-3} \simeq 4. \tag{19}$$

Such a large shift would substantially affect deuterium and lithium predictions and would require a separate BBN calculation within the SU(2)-based thermal history. This possibility is therefore outside the scope of the present CCC+TL consistency test, which assumes the temperature–redshift relation used in the CCC+TL framework.

We have assumed here that the neutron decay rate, governed by the neutron lifetime, is unaffected by covarying coupling constants or changes in the Hubble expansion rate. The neutron lifetime expression is [116]

$$\tau_n = \left(\frac{2\pi^3 \hbar^7}{m_e^5 c^4 f_R} \right) \frac{1}{G_V^2 + 3G_A^2}. \tag{20}$$

Here f_R is a phase-space factor that includes final state and radiative corrections, and m_e is the electron mass. The nucleon vector and axial vector effective weak coupling constants G_V and G_A determine the neutron decay rate and, therefore, the neutron lifetime. The scaling relation for τ_n is not easy to determine in the CCC+TL universe. Nevertheless, using the rate symmetry ansatz mentioned above, the neutron decay rate scales the same as the Hubble rate, i.e., as $\frac{1}{f_{max}}$, and therefore $\tau_n \sim f_{max}$. Alternatively, we may consider that the neutron decay rate is mediated by relativistic particles and thus have the same scaling as H, as we have discussed above. Thus, the proportionality factor $exp\,(\frac{-\Delta t_{cool}}{\tau_n})$ that determines the fraction of neutrons forming elements remains unchanged in CCC+TL cosmology with respect to ΛCDM; the numerator and denominator in the argument of the exponential function are both multiplied by f_{max}, and therefore cancel.

5. Testing with KAWANO/NUC123

We decided to test CCC+TL cosmology with a simple BBN code, Kawano/NUC123 (Hoyle, Wagnor, etc.). It is a well-proven BBN code with limited nuclear reaction data, but it is transparent enough for the modifications required for our purpose. The idea is not to achieve high precision of AlterBBN [117], but to test whether the modifications we have discussed above are meaningful and implementable. The changes made to the NUC123 code (FORTRAN 77/90) are as follows, where fctl $\equiv f_{max}$:

SUBROUTINE rate4(t9): scale reaction rates f(65:88)
f(65:88) = f(65:88)/fctl
Module driver.f
SUBROUTINE start: scale initial time t, timestep dt, and neutron lifetime tau
t = fctl/(const1*uni%t9)**2
dt = fctl*dt1
tau = fctl*tau
SUBROUTINE derivs: scale the expansion rate hubcst
hubcst = hubcst/fctl
SUBROUTINE rate0: divide the (constants) radioactive decay rates by fctl
DO i = 2,11
f(i) = f(i)/fctl
END DO
SUBROUTINE rate1: no addition of any/fctl in f(1) as it is already included through its dependence on tau.
Module reactions.f90
SUBROUTINE rate2(t9): scale reaction rates f(12:34)
f(12:34) = f(12:34)/fctl
SUBROUTINE rate3(t9): scale reaction rates f(35:64)
f(35:64) = f(35:64)/fctl

Reverse reaction rates r are computed elsewhere from forward reaction rates f by detailed balance. Thus, they inherit the same scaling automatically.

Module variables.f90: Declare fctl
REAL, SAVE:: fctl
Module bbn.f90: Read fctl and eta from a .dat file.

The above modifications are all that is needed to test the BBN compliance of the CCC+TL model using the Kawano/NUC123 code. The results we obtain with fctl = 1 (no change, i.e., the ΛCDM model) and fctl = 3 (the CCC+TL model) are the same except for a third or fourth significant figure difference in the elemental abundances, most likely due to numerical rounding errors. Results are presented in Figures 5 and 6.

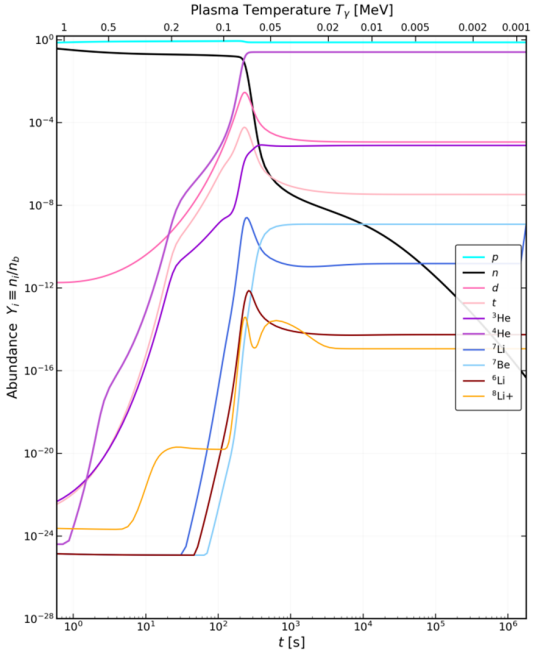


Figure 5. Abundance of light elements' nucleosynthesis with time using the ΛCDM clock. The abundance cut-off was set at 10^{-25}. The temperature scales are the same in the ΛCDL and CCC+TL models, but the clock is three times slower in CCC+TL.

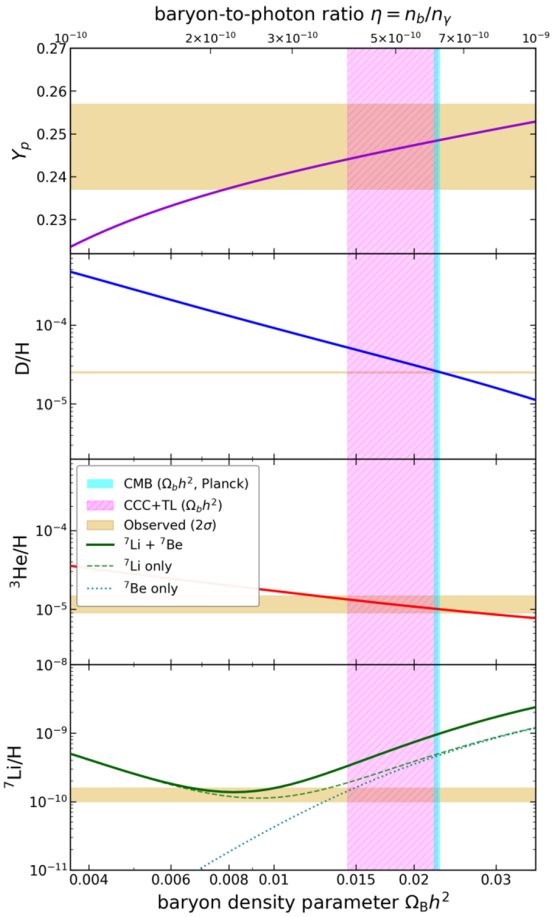


Figure 6. Schramm plot of BBN elemental abundances. The CCC+TL vertical column shows the spread in the values of baryon density calculated using Pantheon+ (lower value edge) and the CMB sound horizon angular size fit (higher value edge). The higher value edge overlaps with the Planck value shown in the light blue narrow vertical band.

6. Discussion

A central requirement for any alternative cosmology is that it preserves the key empirical successes of standard Big Bang nucleosynthesis (SBBN), which links microphysical weak and nuclear reaction kinetics to the macroscopic expansion history and predicts the primordial abundances of D, ^{3}He, ^{4}He, and ^{7}Li with a small set of inputs [8,14,15,35,36]. In the standard BBN, the dominant control parameter is the baryon-to-photon ratio η, with subleading dependence on the expansion rate (often framed via N_{eff}) and the neutron lifetime [33,34,45,46]. The purpose of this work was to assess whether the CCC+TL framework—where only quantities with explicit length dimensionality covary through a single scaling function $f(z)$ while dimensionless constants and ratios remain invariant—remains consistent with these well-tested BBN predictions.

The key simplifying feature for BBN in CCC+TL is that the relevant high-redshift epoch lies on an asymptotic plateau where $f(z) \to f_{max} \approx$ constant, so the model reduces to a global rescaling symmetry for dimensioned quantities. In this regime, the CCC+TL expansion rate satisfies $H_{CTL}(T) = f_{max}^{-1} H_{\Lambda CDM}(T)$, while the temperature–redshift relation retains the standard scaling $T \propto (1+z)$, preserving the thermodynamic milestones (freeze-out and the deuterium bottleneck) at the same temperatures as in ΛCDM.

BBN then reduces to the behavior of *dimensionless* (or effectively dimensionless) governing combinations. First, binding energy thresholds enter as ratios such as $\frac{B_D}{k_B T}$, which remain unchanged because CCC+TL keeps dimensionless ratios invariant by construction. Second, weak freeze-out and related kinetics depend primarily on ratios like $\Gamma_{n\leftrightarrow p}(T)/H(T)$. The scaling argument shows that, on the plateau, reaction/interaction rates inherit the same f_{max}^{-1} factor as H, leaving Γ/H unchanged and therefore preserving the neutron-to-proton ratio at freeze-out. Third, although a smaller H lengthens the cooling interval Δt, this does not change the neutron survival fraction if decay rates (including neutron decay) scale in the same way. In that case the neutron lifetime scales as $\tau_n \propto f_{max}$, so the factor $exp\left(\frac{-\Delta t}{\tau_n}\right)$ remains unchanged. We treat this lifetime scaling as an ansatz, motivated by a broader "rate symmetry" principle and by the fact that BBN is governed mainly by ratios rather than absolute times.

These theoretical expectations are supported by the practical test performed here: implementing the CCC+TL plateau rescalings in Kawano/NUC123 by scaling H, timesteps, and the (assumed) relevant decay/reaction rates by the appropriate powers of f_{max}, we find that the predicted elemental abundances for $f_{max} = 3$ are indistinguishable from the ΛCDM case $f_{max} = 1$ up to ~3rd–4th significant figure differences consistent with numerical rounding. It is worth mentioning that while f_{max} has uncertainties propagating through the uncertainties in α [93,108], they are not relevant for the conclusions reached in this manuscript since f_{max} always approaches a constant value at high redshifts.

Finally, Figure 6 highlights that interpreting BBN constraints in CCC+TL requires care in mapping late-time density parameters to η. Because BBN constraints act primarily on η (not directly on present-day Ω_b definitions), the model remains consistent provided baryon–photon number conservation holds and η is fixed to the recombination value inferred from CMB anisotropies [31,32]. This also clarifies why adopting the lower CCC+TL baryon density estimate may reduce the ^{7}Li discrepancy while simultaneously worsening deuterium, implying that BBN alone does not uniquely select between the late-time baryon density inferences considered here.

BBN is preserved in the CCC+TL cosmology, provided decay and interaction rates obey the same plateau scaling as the Hubble rate H, not necessary based on our pedagogical reasoning. It may be considered as an ansatz or prediction.

7. Conclusions

We conclude that the CCC+TL model is consistent with the BBN-predicted primordial helium and other light-element observations. We show that parameters that determine the abundances of such elements are the same in the CCC+TL and ΛCDM models:

1. Energy ratios and other ratios are dimensionless and therefore are unaffected by covarying coupling constants.
2. Thermodynamics is unchanged; freeze-out and nucleosynthesis temperatures are unaltered.
3. All the rates have scaling symmetry with the Hubble expansion rates, leaving the BBN equations unchanged as they are defined directly or indirectly with respect to the Hubble rate.
4. In comparison to the ΛCDM values, the CCC+TL low-end baryon density reduces the ^{7}Li/H by a factor of ≈ 2.6, i.e., reducing the lithium discrepancy. At the same time, it increases the D/H by a factor of 2, thus creating the deuterium discrepancy. The CCC+TL high-end baryon density is about the same as the ΛCDM value, yielding the same abundances for the two models.
5. We infer that BBN does not constrain either of the two CCC+TL baryon density values, and therefore does not determine preference for either model.

Author Contributions: Conceptualization, R.P.G. and N.S.; methodology, R.P.G.; software, R.P.G.; validation, R.P.G., N.S.; formal analysis, R.P.G.; investigation, R.P.G.; resources, R.P.G.; data curation, R.P.G.; writing—original draft preparation, R.P.G.; writing—review and editing, R.P.G., N.S.; visualization, R.P.G., N.S.; supervision, R.P.G.; project administration, R.P.G.; funding acquisition, R.P.G. All authors have read and agreed to the published version of the manuscript.

Funding: This research received no external funding.

Data Availability Statement: References have been provided for the data used in this work.

Acknowledgments: One of the authors (RPG) is thankful to Alexandre Arbe for multiple email communications regarding the complexity of modifying AlterBBN for the CCC+TL model. He expresses his appreciation to Rodrigo Cuzinatto, Pedro Pompeia, and Piyush Singhal for their discussions on alternative tired light concepts. Authors are grateful to the reviewers for their very constructive comments that resulted in a significant improvement of the paper.

Conflicts of Interest: The authors declare no conflicts of interest.

References

1. Gamow, G. Expanding Universe and the Origin of Elements. *Phys. Rev.* **1946**, *70*, 572. [CrossRef]
2. Alpher, R.A. A Neutron-Capture Theory of the Formation and Relative Abundance of the Elements. *Phys. Rev.* **1948**, *74*, 1577. [CrossRef]
3. Alpher, R.A.; Bethe, H.; Gamow, G. The Origin of Chemical Elements. *Phys. Rev.* **1948**, *73*, 803. [CrossRef]
4. Alpher, R.A.; Herman, R. Theory of the Origin and Relative Abundance Distribution of the Elements. *Rev. Mod. Phys.* **1950**, *22*, 153. [CrossRef]
5. Burbidge, E.M.; Burbidge, G.R.; Fowler, W.A.; Hoyle, F. Synthesis of the Elements in Stars. *Rev. Mod. Phys.* **1957**, *29*, 547. [CrossRef]
6. Cameron, A.G.W. Nuclear Reactions in Stars and Nucleogenesis. *Publ. Astron. Soc. Pac.* **1957**, *69*, 201. [CrossRef]
7. Peebles, P.J.E. Primeval Helium Abundance and the Primeval Fireball. *Phys. Rev. Lett.* **1966**, *16*, 410. [CrossRef]
8. Wagoner, R.V.; Fowler, W.A.; Hoyle, F. On the Synthesis of Elements at Very High Temperatures. *Astrophys. J.* **1967**, *148*, 3. [CrossRef]
9. Weinberg, S. *Gravitation and Cosmology: Principles and Applications of the General Theory of Relativity*; Wiley: New York, NY, USA, 1972.
10. Steigman, G.; Schramm, D.N.; Gunn, J.E. Cosmological limits to the number of massive leptons. *Phys. Lett. B* **1977**, *66*, 202. [CrossRef]

11. Shvartsman, V.F. Density of Relict Particles with Zero Rest Mass in the Universe. *JETP Lett.* **1969**, *9*, 184.
12. Yang, J.; Turner, M.S.; Steigman, G.; Schramm, D.N.; Olive, K.A. Primordial nucleosynthesis: A critical comparison of theory and observation. *Astrophys. J.* **1984**, *281*, 493. [CrossRef]
13. Sarkar, S. Big bang nucleosynthesis and physics beyond the standard model. *Rep. Prog. Phys.* **1996**, *59*, 1493. [CrossRef]
14. Walker, T.P.; Steigman, G.; Schramm, D.N.; Olive, K.A.; Kang, H.-S. Primordial nucleosynthesis redux. *Astrophys. J.* **1991**, *376*, 51. [CrossRef]
15. Olive, K.A.; Steigman, G.; Walker, T.P. Primordial nucleosynthesis: Theory and observations. *Phys. Rep.* **2000**, *333*, 389. [CrossRef]
16. Burles, S.; Nollett, K.M.; Turner, M.S. Big-bang nucleosynthesis predictions for precision cosmology. *Astrophys. J.* **2001**, *552*, L1.
17. Angulo, C.; Arnould, M.; Rayet, M.; Descouvemont, P.; Baye, D.; Leclercq-Willain, C.; Coc, A.; Barhoumi, S.; Aguer, P.; Rolfs, C.; et al. A compilation of charged-particle induced thermonuclear reaction rates. *Nucl. Phys. A* **1999**, *656*, 3. [CrossRef]
18. Dicus, D.A.; Kolb, E.W.; Gleeson, A.M.; Sudarshan, E.C.G.; Teplitz, V.L.; Turner, M.S. Primordial nucleosynthesis including radiative, Coulomb, and finite-temperature corrections to weak rates. *Phys. Rev. D* **1982**, *26*, 2694. [CrossRef]
19. Descouvemont, P.; Adahchour, A.; Angulo, C.; Coc, A.; Vangioni-Flam, E. Compilation and R-matrix analysis of Big Bang nuclear reaction rates. *At. Data Nucl. Data Tables* **2004**, *88*, 203. [CrossRef]
20. Cyburt, R.H. Primordial nucleosynthesis for the new cosmology: Determining uncertainties and examining concordance. *Phys. Rev. D* **2004**, *70*, 023505. [CrossRef]
21. Adelberger, E.G.; Balantekin, A.B.; Bemmerer, D.; Bertulani, C.A.; Chen, J.-W.; Costantini, H.; Couder, M.; Cyburt, R.; Davids, B.; Freedman, S.J.; et al. Solar fusion cross sections II: The pp chain and CNO cycles. *Rev. Mod. Phys.* **2011**, *83*, 195. [CrossRef]
22. Mangano, G.; Miele, G.; Pastor, S.; Pinto, T.; Pisanti, O.; Serpico, P.D. Relic neutrino decoupling including flavour oscillations. *Nucl. Phys. B* **2005**, *729*, 221. [CrossRef]
23. Kawano, L. *Let's Go: Early Universe I. Primordial Nucleosynthesis*; Fermilab-Pub-92/04-A; Fermilab-Pub: Pasadena, CA, USA, 1992.
24. Smith, M.S.; Kawano, L.H.; Malaney, R.A. Experimental, Computational, and Observational Analysis of Primordial Nucleosynthesism. *Astrophys. J. Suppl. Ser.* **1993**, *85*, 219.
25. Pisanti, O.; Cirillo, A.; Esposito, S.; Mangano, G.; Miele, G.; Serpico, P.D. PArthENoPE: Public Algorithm Evaluating the Nucleosynthesis of Primordial Elements. *Comput. Phys. Commun.* **2008**, *178*, 956. [CrossRef]
26. Arbey, A. AlterBBN: A program for calculating the BBN abundances of the elements in alternative cosmologies. *Comput. Phys. Commun.* **2012**, *183*, 1822. [CrossRef]
27. Burles, S.; Tytler, D. The Deuterium Abundance toward Q1937–1009. *Astrophys. J.* **1998**, *499*, 699. [CrossRef]
28. O'Meara, J.M.; Tytler, D.; Kirkman, D.; Suzuki, N.; Prochaska, J.X.; Lubin, D.; Wolfe, A.M. The Deuterium to Hydrogen Abundance Ratio toward a Fourth QSO: HS 0105+1619. *Astrophys. J.* **2001**, *552*, 718. [CrossRef]
29. Pettini, M.; Cooke, R. A new, precise measurement of the primordial abundance of deuterium. *Mon. Not. R. Astron. Soc.* **2012**, *425*, 2477. [CrossRef]
30. Cooke, R.J.; Pettini, M.; Jorgenson, R.A.; Murphy, M.T.; Steidel, C.C. Precision measures of the primordial abundance of deuterium. *Astrophys. J.* **2014**, *781*, 31. [CrossRef]
31. Spergel, D.N.; Verde, L.; Peiris, H.V.; Komatsu, E.; Nolta, M.R.; Bennett, C.L.; Halpern, M.; Hinshaw, G.; Jarosik, N.; Kogut, A.; et al. First-Year Wilkinson Microwave Anisotropy Probe (WMAP) Observations: Foreground Emission. *Astrophys. J. Suppl. Ser.* **2003**, *148*, 175. [CrossRef]
32. Aghanim, N. et al. [Planck Collaboration] Planck 2018 results. VI. Cosmological parameters. *Astron. Astrophys.* **2018**, *641*, A6.
33. Steigman, G. Primordial Nucleosynthesis in the Precision Cosmology Era. *Ann. Rev. Nucl. Part. Sci.* **2007**, *57*, 463. [CrossRef]
34. Fields, B.D. The Primordial Lithium Problem. *Ann. Rev. Nucl. Part. Sci.* **2011**, *61*, 47. [CrossRef]
35. Cyburt, R.H.; Fields, B.D.; Olive, K.A.; Yeh, T.-H. Big bang nucleosynthesis: Present status. *Rev. Mod. Phys.* **2016**, *88*, 015004. [CrossRef]
36. Pitrou, C.; Coc, A.; Uzan, J.-P.; Vangioni, E. Precision big bang nucleosynthesis with improved Helium-4 predictions. *Phys. Rep.* **2018**, *754*, 1–66. [CrossRef]
37. Izotov, Y.I.; Thuan, T.X. The Primordial Abundance of ^{4}He: Evidence for Non-Standard Big Bang Nucleosynthesis. *Astrophys. J.* **2010**, *710*, L67. [CrossRef]
38. Aver, E.; Olive, K.A.; Skillman, E.D. The primordial helium abundance. *J. Cosmol. Astropart. Phys.* **2015**, *7*, 011.
39. Izotov, Y.I.; Thuan, T.X.; Guseva, N.G. A new determination of the primordial helium abundance. *Mon. Not. R. Astron. Soc.* **2014**, *445*, 778.
40. Spite, F.; Spite, M. Abundance of lithium in unevolved stars and old disk stars: Interpretation and consequences. *Astron. Astrophys.* **1982**, *115*, 357.
41. Ryan, S.G.; Beers, T.C.; Olive, K.A.; Fields, B.D.; Norris, J.E. Primordial Lithium and Big Bang Nucleosynthesis. *Astrophys. J.* **2000**, *530*, L57. [PubMed]
42. Asplund, M.; Lambert, D.L.; Nissen, P.E.; Primas, F.; Smith, V.V. Lithium Isotopic Abundances in Metal-poor Halo Stars. *Astrophys. J.* **2006**, *644*, 229. [CrossRef]

43. Sbordone, L.; Bonifacio, P.; Caffau, E.; Ludwig, H.-G.; Behara, N.T.; González Hernández, J.I.; Steffen, M.; Cayrel, R.; Freytag, B.; van't Veer, C.; et al. The metal-poor end of the Spite plateau. I. Stellar parameters, metallicities, and lithium abundances. *Astron. Astrophys.* **2010**, *522*, A26.
44. Wagoner, R.V. Synthesis of the Elements within Objects Exploding from Very High Temperatures. *Astrophys. J. Suppl. Ser.* **1969**, *18*, 247. [CrossRef]
45. Coc, A.; Vangioni, E. Primordial nucleosynthesis. *Int. J. Mod. Phys. E* **2017**, *26*, 1741002.
46. Fields, B.D.; Olive, K.A.; Yeh, T.-H.; Young, C. Big-Bang Nucleosynthesis after Planck. *J. Cosmol. Astropart. Phys.* **2020**, *3*, 10.
47. Dirac, P.A.M. The Cosmological Constants. *Nature* **1937**, *139*, 3512. [CrossRef]
48. Gilbert, C. The gravitational field of a star in the expanding universe. *Mon. Not. R. Astron. Soc.* **1956**, *116*, 678.
49. Gilbert, C. Dirac's Cosmology. *Nature* **1961**, *192*, 4797. [CrossRef]
50. Canuto, V.; Lodenquai, J. Dirac cosmology. *Astrophys. J.* **1977**, *211*, 342–356. [CrossRef]
51. Maeder, A. MOND as a peculiar case of the SIV theory. *Mon. Not. R. Astron. Soc.* **2023**, *520*, 1447–1455. [CrossRef]
52. Maeder, A. Scale-invariant Cosmology and CMB Temperatures as a Function of Redshifts. *Astrophys. J.* **2017**, *847*, 65. [CrossRef]
53. Maeder, A. Evolution of the early Universe in the scale invariant theory. *arXiv* **2019**, arXiv:1902.10115.
54. Brans, C.; Dicke, R.H. Mach's Principle and a Relativistic Theory of Gravitation. *Phys. Rev.* **1961**, *124*, 3. [CrossRef]
55. Weyl, H. *Space, Time, Matter*; Brose, H.L., Translator; Dover Publications: Mineola, NY, USA, 1952.
56. Romero, C.; Fonseca-Neto, J.B.; Pucheu, M.L. General relativity and Weyl geometry Class. *Quant. Grav.* **2012**, *29*, 15.
57. Cuzinatto, R.R.; Gupta, R.P.; Pompeia, P.J. Dynamical Analysis of the Covarying Coupling Constants in Scalar–Tensor Gravity. *Symmetry* **2023**, *15*, 709. [CrossRef]
58. Teller, E. On the Change of Physical Constants. *Phys. Rev.* **1948**, *73*, 801. [CrossRef]
59. Chin, C.-W.; Stothers, R. Limit on the Secular Change of the Gravitational Constant Based on Studies of Solar Evolution. *Phys. Rev. Lett.* **1976**, *36*, 833. [CrossRef]
60. Sahini, V.; Shtanov, Y. Can a variable gravitational constant resolve the faint young Sun paradox? *Int. J. Mod. Phys. D* **2014**, *23*, 1442018. [CrossRef]
61. Morrison, L.V. Rotation of the Earth from AD 1663–1972 and the Constancy of *G*. *Nature* **1973**, *241*, 519. [CrossRef]
62. Sisterna, P.; Vucetich, H. Cosmology, oscillating physics, and oscillating biology. *Phys. Rev. Lett.* **1994**, *72*, 454. [CrossRef]
63. Benvenuto, O.G.; Althaus, L.G.; Torres, D.F. Evolution of white dwarfs as a probe of theories of gravitation: the case of Brans–Dicke. *Mon. Not. R. Astron. Soc.* **1999**, *305*, 905.
64. García-Berro, E.; Lorén-Aguilar, P.; Torres, S.; Althaus, L.G.; Isern, J. An upper limit to the secular variation of the gravitational constant from white dwarf stars. *J. Cosm. Astropart. Phys.* **2011**, *5*, 21.
65. Córsico, A.H.; Romero, A.D.; Althaus, L.G.; García-Berro, E.; Isern, J.; Kepler, S.O.; Miller Bertolami, M.M.; Sullivan, D.J.; Chote, P. An asteroseismic constraint on the mass of the axion from the period drift of the pulsating DA white dwarf star L19-2. *J. Cosm. Astropart. Phys.* **2013**, *6*, 32.
66. degl'Innocenti, S.; Fiorentini, G.; Raffelt, G.G.; Ricci, B.; Weiss, A. Time-variation of Newton's constant and the age of globular clusters. *Astron. Astrophys.* **1995**, *312*, 345. [CrossRef]
67. Thorsett, S.E. The Gravitational Constant, the Chandrasekhar Limit, and Neutron Star Masses. *Phys. Rev. Lett.* **1996**, *77*, 1432. [CrossRef] [PubMed]
68. Bai, Y.; Salvado, J.; Stefanek, B.A.J. Bounds on varying fundamental constants from big bang nucleosynthesis. *Cosm. Astropart. Phys.* **2015**, *15*, 29.
69. Ooba, J.; Ichiki, K.; Chiba, T.; Sugiyama, N. Cosmological constraints on scalar-tensor gravity and the variation of the gravitational constant. *Prog. Theor. Exp. Phys.* **2017**, *43*, E03.
70. Copi, C.J.; Davis, A.N.; Krauss, L.M. New Nucleosynthesis Constraint on the Variation of *G*. *Phys. Rev. Lett.* **2004**, *92*, 171301. [CrossRef] [PubMed]
71. Alvey, J.; Sabti, N.; Escudero, M.; Fairbairn, M. Improved BBN constraints on the variation of the gravitational constant. *Eur. Phys. J. C* **2020**, *80*, 148. [CrossRef]
72. Bellinger, E.P.; Christensen-Dalsgaard, J. Asteroseismic Constraints on the Cosmic-time Variation of the Gravitational Constant from an Ancient Main-sequence Star. *Astrophys. J. Lett.* **2019**, *887*, L1. [CrossRef]
73. Williams, J.G.; Turyshev, S.G.; Boggs, D.H. Progress in Lunar Laser Ranging Tests of Relativistic Gravity. *Phys. Rev. Lett.* **2004**, *93*, 261101. [CrossRef] [PubMed]
74. Hofmann, F.; Müller, J. Relativistic tests with lunar laser ranging. *Müller Class. Quant. Grav.* **2018**, *35*, 035015. [CrossRef]
75. Pitjeva, E.V.; Pitjev, N. Relativistic effects and dark matter in the Solar system from observations of planets and spacecraft. *Mon. Not. R. Astron. Soc.* **2013**, *432*, 3431. [CrossRef]
76. Fienga, A.; Laskar, J.; Exertier, P.; Manche, H.; Gastineau, M. Numerical estimation of the sensitivity of INPOP planetary ephemerides to general relativity parameters. *Celest. Mech. Dyn. Astron.* **2015**, *123*, 325–349. [CrossRef]

77. Genova, A.; Mazarico, E.; Goossens, S.; Lemoine, F.G.; Neumann, G.A.; Smith, D.E.; Zuber, M.T. Solar system expansion and strong equivalence principle as seen by the NASA MESSENGER mission. *Nat. Commun.* **2018**, *9*, 289. [CrossRef] [PubMed]
78. Damour, T.; Gibbons, G.W.; Taylor, J.H. Limits on the variability of *G* using binary-pulsar data. *Phys. Rev. Lett.* **1988**, *61*, 1151. [PubMed]
79. Kaspi, V.M.; Taylor, J.H.; Ryba, M. High-Precision Timing of Millisecond Pulsars. III. Long-Term Monitoring of PSRs B1855+09 and B1937+21. *Astrophys. J.* **1994**, *428*, 713. [CrossRef]
80. Zhu, W.W.; Desvignes, G.; Wex, N.; Caballero, R.N.; Champion, D.J.; Demorest, P.B.; Ellis, J.A.; Janssen, G.H.; Kramer, M.; Krieger, A.; et al. Tests of gravitational symmetries with pulsar binary J1713+0747. *Mon. Not. R. Astron. Soc.* **2019**, *482*, 3249.
81. Gaztañaga, E.; García-Berro, E.; Isern, J.; Bravo, E.; Domínguez, I. Bounds on the possible evolution of the gravitational constant from cosmological type-Ia supernovae. *Phys. Rev. D* **2001**, *65*, 023506. [CrossRef]
82. Wright, B.S.; Li, B. Type Ia supernovae, standardizable candles, and gravity. *Phys. Rev. D* **2018**, *97*, 083505. [CrossRef]
83. Einstein, A. On the Relativity Principle and the Conclusions Drawn from It (Jahrbuch fur Radioaktivitat und Elektronik). *Yearb. Radioact. Electron. (Jahrb. Der Radioakt. Und Elektron.)* **1907**, *4*, 11.
84. Dicke, R.H. Gravitation without a Principle of Equivalence. *Rev. Mod. Phys.* **1957**, *29*, 363. [CrossRef]
85. Petit, J.-P. An Interpretation of Cosmological Model With Variable Light Velocity. *Mod. Phys. Lett. A* **1988**, *3*, 1527; ibid 1733; ibid 2201. [CrossRef]
86. Moffat, J.W. Superluminary Universe: A Possible Solution to the Initial Value Problem in Cosmology. *Int. J. Mod. Phys. D* **1993**, *2*, 351. [CrossRef]
87. Moffat, J.W. A new theory of gravitation. *Found. Phys.* **1993**, *23*, 411.
88. Albrecht, A.; Magueijo, J. A time-varying speed of light as a solution to cosmological puzzles. *Phys. Rev. D* **1999**, *59*, 043516.
89. Barrow, J.D. Cosmologies with varying light speed. *Phys. Rev. D* **1999**, *59*, 043515. [CrossRef]
90. Avelino, P.P.; Martins, C.J.A.P. Does a varying speed of light solve the cosmological problems? *Phys. Lett. B* **1999**, *459*, 468. [CrossRef]
91. Avelino, P.P.; Martins, C.J.A.P.; Rocha, G. VSL theories and the Doppler peak. *Phys. Lett. B* **2000**, *483*, 210. [CrossRef]
92. Moffat, J.W. Variable speed of light cosmology, primordial fluctuations and gravitational waves. *Eur. Phys. J. C* **2016**, *76*, 130. [CrossRef]
93. Gupta, R.P. Testing CCC+TL Cosmology with Observed Baryon Acoustic Oscillation Features. *Astrophys. J.* **2024**, *964*, 55. [CrossRef]
94. Gupta, R.P. On Dark Matter and Dark Energy in CCC+TL Cosmology. *Universe* **2024**, *10*, 266. [CrossRef]
95. Gupta, R.P. Testing CCC+TL Cosmology with Galaxy Rotation Curves. *Galaxies* **2025**, *13*, 108. [CrossRef]
96. Gupta, R.P. Evolution of Size, Mass, and Density of Galaxies Since Cosmic Dawn. *Galaxies* **2025**, *13*, 115. [CrossRef]
97. Cuzinatto, R.R. Joint Primordial Nucleosynthesis and Cosmic Microwave Background Bounds on Varying Fundamental Constants. *Phys. Lett. A* **2026**. *to be published*.
98. Hofmann, R.; Meinert, J.; Balaji, S.S. Cosmological Parameters from Planck Data in SU(2)CMB, Their Local ΛCDM Values, and the Modified Photon Boltzmann Equation. *Ann. Der Phys.* **2023**, *535*, 2200517. [CrossRef]
99. Rabinowitch, A.S. Big Bang nucleosynth'esis with varying fundamental constants. *Nucl. Phys. B* **2017**, *1001*, 116505.
100. Kaluza, T. On the Unification Problem in Physics. *Int. J. Mod. Phys. D* **2018**, *27*, 1870001. [CrossRef]
101. Sakharov, A.D. Violation of CP invariance, C asymmetry, and baryon asymmetry of the universe. *JETP Lett.* **1967**, *5*, 24.
102. Overduin, J.M.; Wesson, P.S. Kaluza–Klein gravity. *Phys. Rep.* **1997**, *283*, 303. [CrossRef]
103. Padmanabhan, T. Cosmological constant—The weight of the vacuum. *Rep. Prog. Phys.* **2010**, *73*, 046901.
104. Damour, T.; Polyakov, A.M. The string dilaton and a least coupling principle. *Nucl. Phys. B* **1994**, *423*, 532. [CrossRef]
105. Uzan, J.-P. The fundamental constants and their variation: Observational and theoretical status. *Rev. Mod. Phys.* **2003**, *75*, 403. [CrossRef]
106. Martins, C.J.A.P. The status of varying constants: A review. *Rep. Prog. Phys.* **2017**, *80*, 126902. [CrossRef] [PubMed]
107. Gupta, R.P. JWST early Universe observations and ΛCDM cosmology. *Mon. Not. R. Astron. Soc.* **2023**, *524*, 3385–3395. [CrossRef]
108. Gupta, R.P. Testing CCC+TL Cosmology with Observed Baryon Acoustic Oscillation Features. *Astroph. J.* **2024**, *964*, 55. [CrossRef]
109. Gupta, R.P. Evolution of Size, Mass, and Density of Galaxies Since Cosmic Dawn. *Galaxies* **2025**, *13*, 115. [CrossRef]
110. Gupta, R.P. Testing CCC+TL Cosmology with Galaxy Rotation Curves. *Galaxies* **2025**, *13*, 108. [CrossRef]
111. Scolnic, D.M.; Jones, D.O.; Rest, A.; Pan, Y.C.; Chornock, R.; Foley, R.J.; Huber, M.E.; Kessler, R.; Narayan, G.; Riess, A.G.; et al. The Complete Light-curve Sample of Spectroscopically Confirmed SNe Ia from Pan-STARRS1 and Cosmological Constraints from the Combined Pantheon Sample. *Astrophys. J.* **2018**, *859*, 101.
112. Brout, D.; Scolnic, D.; Popovic, B.; Riess, A.G.; Carr, A.; Zuntz, J.; Kessler, R.; Davis, T.M.; Hinton, S.; Jones, D.; et al. The Pantheon+ Analysis: Cosmological Constraints. *Astrophys. J.* **2022**, *938*, 110. [CrossRef]
113. Bernstein, J.; Brown, L.S.; Feinberg, G. Cosmological helium production simplified. *Rev. Mod. Phys.* **1989**, *61*, 25. [CrossRef]
114. Kolb, E.W.; Turner, M.S. *The Early Universe*; Addison-Wesley: Reading, MA, USA, 1990.

115. Hahn, S.; Hoffman, R. Varying fine-structure constant in big bang nucleosynthesis. *Mod. Phys. Lett. A* **2017**, *33*, 1850029.
116. Wietfeldt, F.E. The Neutron Lifetime. *arXiv* **2014**, arXiv:1411.3687v1.
117. Arbey, A.; J. Auffinger, J.; Hickerson, K.P.; Jenssen, E.S. AlterBBN v2: A public code for calculating Big-Bang nucleosynthesis abundances in alternative cosmological models. *arXiv* **2018**, arXiv:1806.11095.

Disclaimer/Publisher's Note: The statements, opinions and data contained in all publications are solely those of the individual author(s) and contributor(s) and not of MDPI and/or the editor(s). MDPI and/or the editor(s) disclaim responsibility for any injury to people or property resulting from any ideas, methods, instructions or products referred to in the content.